Jordan Journal of Civil Engineering, Volume **18**, No. **3**, **2024**
DOI: https://doi.org/10.14525/JJCE.v18i3.13

Jordan Journal of Civil Engineering

Journal homepage: https://jjce.just.edu.jo

Static Analysis of Functionally Graded Beams under Bending Using a New Polynomial Shear Function

Aissa Boussouar [1]**,** ***Bachir Taallah*** [2]**,** ***Ali Zaidi*** [3]*

[1] *PhD Student, Civil Engineering Research Laboratory, Mohamed Khider University of Biskra, Biskra, Algeria, E-Mail: Batiaissa85@gmail.com*
[2] *Professor, Department of Civil Engineering and Hydraulics, Civil Engineering Research Laboratory, Mohamed Khider University of Biskra, Algeria. E-Mail: b.taallah@gmail.com*
[3] *Professor, Structures Rehabilitation and Materials Laboratory (SREML), University of Laghouat, BP 37G, 03000, Laghouat, Algeria. Associate Professor, Department of Civil and Building Engineering, University of Sherbrooke, Sherbrooke, QC., Canada. * Corresponding Author. E-Mails: a.zaidi@lagh-univ.dz; Ali.Zaidi@USherbrooke.ca*

ARTICLE INFO

Article History:
Received: 7/11/2023
Accepted: 21/6/2024

ABSTRACT

This paper presents a static analysis to establish a mathematical model using high-order bending theories to predict the shear strain in the displacement fields for functionally graded beams under bending. The new polynomial shear function developed, which represents the originality of this research work, satisfies the boundary conditions and stress nullities on the lower and upper faces of the section through the thickness. This new model, considering a hyperbolic shape function, does not need a shear correction factor. The material properties are assumed to vary continuously in the thickness direction, based on a simple power-law distribution, in terms of constituent volume fractions. The analytical model is developed by differential equations obtained from the virtual work principle as well as equilibrium equations and boundary conditions considered. The solution model is based on an integral approach to evaluate the displacement field component and the basic constitutive laws. The analytical model is explored using the illustrative case. The results obtained in terms of displacement field including shear strains and shear stresses predicted from the proposed model are compared to those obtained from the literature.

Keywords: Higher-order theories, Beams, Displacement, Static analysis, New polynomial shear function, Shear stress.

INTRODUCTION

Functionally graded materials (FGMs) developed by Japanese scientists were made, in general, from a mixture of ceramics and metals for their best physical and mechanical properties (thermal resistance of ceramic and high strength of metal). Therefore, these materials were used in many structures, such as aeronautic, automotive, and civil constructions. Numerous research works were carried out to investigate the behavior of FGM structures. Guenfoud et al. (2016) and Ziou et al. (2021) proposed new polynomial shear functions that satisfied the stress-free boundary conditions. However, these theories had strong similarities with Timoshenko beam theory in some concepts, such as equations of movement, boundary conditions and stress resultant expressions. Ghugal et al. (2011-2012) developed a shear deformation theory, taking into account transverse shear deformation effects, for the static flexural analysis of thick isotropic beams of rectangular cross-section with various boundaries and loading (concentrated and uniformly) conditions. The authors compared the displacement field of illustrative cases to those of Timoshenko and other solutions. Also, beams were subjected to parabolic and cosine loads. Variations of axial displacement, axial stress and transverse shear stress, were validated. Gandhe et al. (2018) studied the static flexural analysis of thick beams using the hyperbolic shear deformation theory.

The virtual work principle was used to derive the governing equations of beams. Displacements and stresses obtained for beams under variable loads were compared to those predicted from Timoshenko and higher-order theories. Benatta et al. (2008) investigated the flexural response of short hybrid composite beams varying fiber spacing. The authors proved that the hybrid functionally graded material (FGM) with a fiber volume fraction variation could improve the beam performance. Kadoli et al. (2008) carried out an investigation on the static analysis of functionally graded beams composed with the metal–ceramic combination under uniformly distributed load using the higher-order shear deformation theory. The finite-element form of static equilibrium equation for FGM beam was developed using the principle of stationary potential energy to determine the transverse deflection, as well as axial and shear stresses in a moderately thick FGM beam based on the higher-order shear deformation theory. The numerical results showed that the deflections, stresses and the location of the neutral surface depended mainly on the power law index. Lu et al. (2008) performed a study on bending and thermal deformations of functionally graded beams with various end conditions, using the hybrid state space-based differential quadrature method (DQM) and the state space method (SSM). The main results showed that the appropriate selection of material properties against temperature load was able to reduce thermal stresses. The distribution of axial normal and transverse shear stresses obtained using the semi-analytical method and the finite element method (FEM), the effect of gradient indices on the deformation and the stress distribution, were presented. Aydogdu et al. (2007) studied the free vibration analysis of functionally graded beams, governing equations by Hamilton's principle and Navier type solution to obtain frequencies of FG beams with simply supported ends. The classical beam theory (CBT) gave higher results; furthermore, the difference between the CBT and higher order theories increased with increasing the mode number. Mengzhen et al. (2020) investigated FG plate simply supported boundary with a new generalized five-variable shear deformation theory developed and an exponential function with a classical trigonometric shear strain shape function to make an accurate distribution of the transverse shear strain. Hamilton principle was used for deriving the governing differential equations. The main results predicted with the novel transverse shear function were more precise compared to those obtained with other higher-shear deformation theories. Reddy (1984) analyzed and proposed a new polynomial shear function for laminated composite plates using a simple higher order theory. Deflections and stresses predicted from the developed theory were more accurate compared to those determined from the first-order theory. Sayyad et al. (2011) suggested a new hyperbolic shear deformation for the static flexure of the thick isotropic beam satisfying the shear stress free surface conditions on the top and the bottom of the beam theory. An analytical model was developed by differential equations obtained from the virtual work principle and boundary conditions, where three illustrative examples, subjected to single sine load, uniformly distributed load and linearly variable load to determine displacements and stresses, were analyzed. It is important to note that the theory suggested by the authors did not need the shear correction factor. Simsek et al. (2009) analyzed a functionally graded simply-supported beam subjected to a uniformly distributed load using the Ritz method. The axial and the transverse displacements, as well as the rotation of the cross-sections of the FGM beam were expressed in the trigonometric functions. The material properties of the beam were considered variable through the thickness according to the power-law form. The numerical results showed that the modulus of elasticity played a major role in the displacements and the stress distributions of the FGM beam. In addition, the shear stress distributions were more affected by the chosen power-law exponent. Li (2008) analyzed the static and dynamic behaviors of functionally graded beams with the rotary inertia and shear deformation included. The author showed that for the two cases (static and dynamic), the Rayleigh and Euler–Bernoulli beam theories could be analytically reduced from the Timoshenko beam theory. A ratio in term of the deflection solution between the Timoshenko beam theory and Rayleigh and the Euler–Bernoulli beam theories *versus* the proposed index and a comparison of three mode shapes of vibration of a cantilever beam subjected to uniform and concentrated loads, were investigated. Zaoui et al. (2017) presented an analytical solution for free vibration behavior of functionally graded (FG) beams using a refined hyperbolic function of shear deformation theory including the stretching effects. Equations were derived by Hamilton's principle and Navier-type solutions. In addition, the authors analyzed the effect of the slenderness ratio and the material gradient parameters on the natural frequencies for FG-beam simply supported ends. The results obtained proved that the effect of the shear deformation on the frequencies had a tendency to be more significant when the beams became shorter. Zheng et al. (2007) exhibited expressions of analytical two-dimensional elasticity solutions for a functionally graded (FG) cantilever beam subjected to different loads (normal and shear tractions, concentrated forces and couple) under different boundary conditions. The results showed that the proposed solutions could be used to analyze the FG-beam and could serve as a basis for establishing simplified FG beam theories. Ziou et al. (2016) analyzed a cantilever functionally graded material (FGM) beam subjected to a concentrated force at the free end for different (length-to-thickness) ratios chosen using the finite element method. The governing equations and boundary conditions were derived from the virtual work principle. The numerical results proved that deflections were higher for metal rich beams compared to those of ceramic rich beams. Furthermore, the deflection increased as the power law index increased. In addition, the Timoshenko beam theory was used to examine deflections, stress distribution, and strains on the beam. However, these previous research works as seen in this literature review did not investigate sufficiently the FG beams. For this reason, a new polynomial shear function is developed, in this study, for the shear deformations in the displacement field. This developed analytical model is a new contribution not used elsewhere. The numerical results, in terms of displacement field, stresses, and deformations, predicted from the developed model are compared with those published in the literature for simply supported beams.

BEAM THEORIES AND PROPERTIES

Beam Theories

Considering the geometric dimensions of the beam at the boundary restrains, as shown in Figure 1, having the span length (L), the width (b), and the total thickness (h), where x, y and z are the Cartesian coordinates with intervals cited below:

$$0 \leq x \leq L\,; -\frac{b}{2} \leq y \leq \frac{b}{2}\;\; ; -\frac{h}{2} \leq z \leq \frac{h}{2}.$$

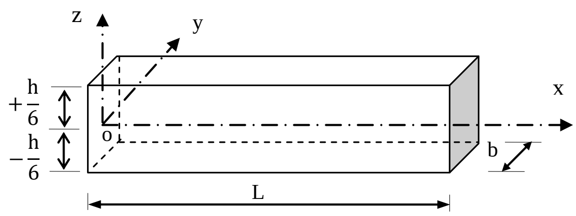

Figure (1): Geometry of beams

Briefly, the normal transverse and shear effects are negligible according to the assumption of the Euler-Bernoulli classical beam theory (CBT) which considers that the cross-sections normal to the mid surface before deformation remain straight and normal to the median surface after deformation. Therefore, there is no shape function used in this theory (CBT). Timoshenko's theory includes the cross-section deformation (shear deformation effect) added to the displacement fields with a linear shape function. New higher-order shear strain theories, including shape functions and stress nullities at the bottom and top faces of the section through the beam thickness, are used. These theories do not require a shear correction coefficient contrary to the Timoshenko's beam theory, as well as to the Euler-Bernoulli classical beam theory (CBT).

Material Properties

Equations (1) and (2) depict the constituent mixture between ceramic volume fraction V_c and metal volume fraction V_m when a simple power law is drawn in Figure 2 as follows:

$$V_c = \left(\frac{z}{h} + \frac{1}{2}\right)^{p} \qquad (1)$$

$$V_m = 1 - V_c \qquad (2)$$

The effective stiffness coefficients $E_{eff}(z)$ and $G_{eff}(z)$ obtained based on the mixture rule of constituents, can be written as follows:

$$E_{eff} = (E_c - E_m)\left(\frac{z}{h}+\frac{1}{2}\right)^p + E_m \quad (3)$$

$$G_{eff} = (G_c - G_m)\left(\frac{z}{h}+\frac{1}{2}\right)^p + G_m \quad (4)$$

Also, the effective Poisson's ratio υ_{eff} is presented below:

$$\upsilon_{eff} = (\upsilon_c - \upsilon_m)\left(\frac{z}{h}+\frac{1}{2}\right)^p + \upsilon_m \quad (5)$$

The effective Poisson's ratio is varied from 0.25 to 0.3. P is the power index which describes the profile variation of materials depending on the thickness.

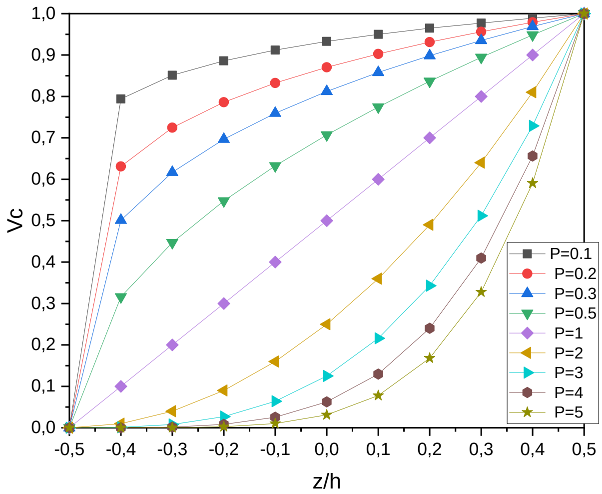

Figure (2): Variation of volume fraction of ceramic (V_c) *versus* (z/h) ratio and the power law index (P)

Cross-section Properties

Equations (6), (7) and (8) are the stiffness coefficients of beam; namely, extension, bending-extension coupling, and bending stiffness coefficients, respectively. Their expressions are given by:

$$D_{aa} = b\int_{-\frac{h}{2}}^{\frac{h}{2}} E(z)\,dz = bh\left(E_m + \frac{E_c - E_m}{p+1}\right) \quad (6)$$

$$D_{ab} = b\int_{-\frac{h}{2}}^{\frac{h}{2}} E(z)z\,dz = \frac{bh^2}{2}(E_c - E_m)\left[\frac{p}{(p+1)(p+2)}\right] \quad (7)$$

$$D_{bb} = b\int_{-\frac{h}{2}}^{\frac{h}{2}} E(z)z^2\,dz = \frac{bh^2}{12}\left[3(E_c - E_m)\frac{p^2+p+2}{(p+3)(p+2)(p+1)}\right] \quad (8)$$

Also, the coefficient of the transverse shear stiffness is presented as follows:

$$D_S = k_z b\int_{-\frac{h}{2}}^{\frac{h}{2}} G(z)dz \quad (9)$$

where, k_z is the shear correction factor for bending.

Equation (10) presents the neutral axis position from the thickness of the beam given by:

$$h_0 = \frac{D_{ab}}{D_{aa}} = \frac{\int_{-\frac{h}{2}}^{\frac{h}{2}} E(z)z\,dz}{\int_{-\frac{h}{2}}^{\frac{h}{2}} E(z)dz} \quad (10)$$

Differential Equations and Boundary Conditions

Considering the geometric dimensions of the beam at the boundary restrains, as shown in Figure 3, having a width (b), a span length (L), a thickness (h), an inertia (I), under transverse distributed uniform load (q), in this section, it can be noted that only a pure flexure is reported.

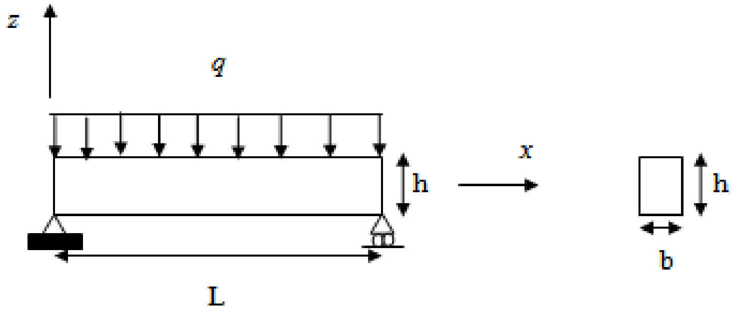

Figure (3): Simply supported beam subjected to a uniformly distributed load q

The virtual work principle applied in brief on the beam is defined as follows:

$$b\int_{x=0}^{x=L}\int_{z=\frac{-h}{2}}^{z=\frac{h}{2}}(\sigma_x\delta\varepsilon_x+\tau_{xz}\delta\gamma_{xz})dxdz-\int_{x=0}^{x=L}q\delta w dx=0 \quad (11)$$

where, σ_x is the normal stress; τ_{xz} is the shear stress; $\delta\varepsilon_x$ is the incremental normal strain; $\delta\gamma_{xz}$ is the incremental shear strain.

Thus, Equation (11) can be rewritten as:

$$b\int_{x=0}^{x=L}\left(N\frac{\partial\delta u_0}{\partial x}-M_b\frac{\partial^2\delta w_0}{\partial x^2}+M_s\frac{\partial\delta\psi_x}{\partial x}+Q\delta\psi_x\right)dx-b\int_{x=0}^{x=L}q\delta w_0 dx=0 \quad (11-a)$$

where, δu_0, $\delta\psi_x$ and δw_0, are the incremental normal displacement, shear strain and transverse displacement of the beam, respectively.

Equations (11-b) and (11-c) present the normal resultant force (N) and the shear resultant force (Q), respectively.

$$N=\int_{\frac{-h}{2}}^{\frac{h}{2}}\sigma_x dz \quad (11-b)$$

$$Q=\int_{\frac{-h}{2}}^{\frac{h}{2}}\frac{\partial\varphi(z)}{\partial z}\tau_{zx}dz \quad (11-c)$$

The resultant moments M_b and M_s presented by Equations (11-d) and (11-e), respectively, are given by:

$$M_b=\int_{\frac{-h}{2}}^{\frac{h}{2}}z\sigma_x dz \quad (11-d)$$

$$M_s=\int_{\frac{-h}{2}}^{\frac{h}{2}}\varphi(z)\sigma_x dz \quad (11-e)$$

where $\varphi(z)$ is the shape function.

Equilibrium Equations from (12) to (15) are derived by deductions from the integrals:

$$\frac{\partial N(x)}{\partial x}=0 \quad (12)$$

$$\frac{\partial^2 M_b}{\partial x^2}+q=0 \quad (13)$$

$$\frac{\partial^2 M_s}{\partial x^2}+\frac{\partial Q}{\partial x}+q=0 \quad (14)$$

$$\frac{\partial M(x)}{\partial x}-N(x)=0 \quad (15)$$

In addition, the application of essential boundary conditions of Neumann (at x = L/2, $\partial w(x=L/2)/\partial x = 0$) and natural boundary conditions of Dirichlet (at x = 0, $w(x=0) = 0$ and $\psi_x(x=L/2) = 0$) for the considered case, is as shown below.

-Case: Boundary conditions of beam with uniformly distributed load (q)

$$D^*_{11}\frac{\partial^3 w(x)}{\partial x^3}=D^*_{11}\frac{\partial^2\varphi_x}{\partial x^2}=\frac{\partial w}{\partial x}=\varphi_x=0 \text{ for } x=\frac{L}{2} \quad (16)$$

$$D^*_{11}\frac{\partial^2 w(x)}{\partial x^2}=\frac{\partial\varphi_x}{\partial x}=w=0 \text{ for } x=0 \text{ and } x=L \quad (17)$$

where, $D^*_{11}=\frac{b}{E_x I}$ is the bending stiffness constant of the beam.

The equilibrium equation can be written as shown below.

$$\frac{\partial^2\varphi_x}{\partial x^2}-\frac{D^*_{11}}{F^*_{55}}\left(\varphi_x+\frac{\partial w_0(x)}{\partial x}\right)=0 \qquad (18)$$

Also,

$$\frac{\partial^2 w(x)}{\partial x^2}+\frac{\partial\varphi_x}{\partial x}+F^*_{55}q=0 \qquad (18-a)$$

MATHEMATICAL MODEL

Displacement Field

The displacement components are defined from Equations (19) to (21) along x and z directions of the beam given as below:

$$u(x,z)=u_0(x)-z\frac{\partial w_0}{\partial x}+\varphi(z)\psi_x \qquad (19)$$

$$v(x,z)=0 \qquad (20)$$

$$w(x,z)=w_0(x) \qquad (21)$$

where u_0 and w_0 are the axial and the transverse displacements on the mid-plane.

The higher-order theories include also the transverse deformation (shear deformation effect) added to the displacement field with non-linear shape function *φ(z)*.

where, $\varphi(z)\psi_x$ depicts the deformation function.

The shear coefficient S is defined by the following equation:

$$S=\frac{E_x}{G_{xz}}\left(\frac{h}{L}\right)^2=12\frac{F^*_{55}}{D^*_{11}}\left(\frac{h}{L}\right)^2 \qquad (22)$$

where, $F^*_{55}=\frac{1}{hG_{xz}}$ is the shear stiffness constant of the beam.

Along x and z directions of the beam, as shown in Figure 4, the transverse expression of the displacement is presented by the following equation:

$$w_0(x)=-\frac{qL^4}{4E_xbh^3}\left(2\frac{x^4}{L^4}+\frac{x}{L}+S\right) \qquad (23)$$

The maximum value is evaluated at (x=L/2) as follows:

$$w_c\left(x=\frac{L}{2}\right)=-\frac{qL^4}{4E_xbh^3}\left(\frac{5}{8}+S\right) \qquad (23-a)$$

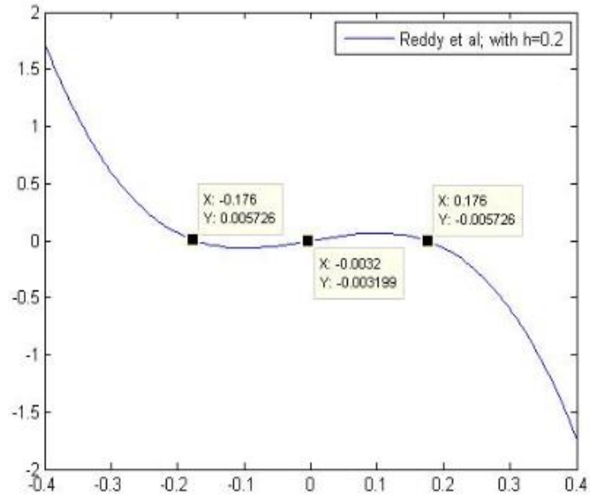

Figure (4): Reddy's analytical function curve with square root point solutions

New Polynomial Shear Function

A new polynomial shear function contribution is proposed in this section. This function is given as below:

$$\varphi(z)=z\left(\frac{13}{12}-\frac{13z^2}{9h^2}\right) \qquad (24)$$

At both top and bottom fibers where ($z=\pm\frac{h}{2}$), the first derivative of polynomial shear function $\frac{\partial\varphi(z)}{\partial z}=0$. In addition, the nullity of the shear stress can be confirmed at these fibers.

$$\frac{\partial\varphi(z)}{\partial z}=\frac{13}{12}-\frac{13z^2}{3h^2} \qquad (24-a)$$

The second derivative for (z=0) involves that the shear stress is maximal at the midline fiber, when φ (z=0) =0.

$$\frac{\partial^2\varphi(z)}{\partial z^2}=-\frac{26\,z}{3h^2} \qquad (24-b)$$

The newly proposed shear function is compared to the parabolic shear deformation beam theories (PSDBT) suggested by Reddy (1984) and Guenfoud et al. (2016), respectively.

Substituting the shear function expression (Eq. 24) into Equation (19), then after simplification, we obtain the following equation:

$$u(x,z)=u_0(x)-z\left(\frac{\partial w_0}{\partial x}-\frac{13}{12}\psi_x\right)-\frac{13z^3}{9h^2}\psi_x \qquad (25)$$

This equation (Eq .25) is close to the following equations (Eq. 25-a, 25-b) developed by Reddy (1984) for higher-order shear deformation theories (HSDTs).

$$u(x,z) = u_0(x) + zu_1(x) + z^2u_2(x) + z^3u_3(x) \quad (25\text{-a})$$

Because the shear stress is zero on the two fibers of the beam (±h/2), the relation between the shear strain and stress must vanish the shear strain, thus $u_2(x)=0$.

Therefore, Equation (25-a) becomes:

$$u(x,z) = u_0(x) + zu_1(x) + z^3u_3(x) \quad (25\text{-b})$$

EQUATIONS OF STRAIN COMPONENTS

From the mathematical derivation of the displacement field (Eq. 19), we obtain the normal strain as given by the following expression:

$$\varepsilon_x(x,z) = \frac{\partial u_0}{\partial x} - z\frac{\partial^2 w_0}{\partial x^2} + \varphi(z)\frac{\partial\,\psi_{\mathbf{x}}}{\partial x} \quad (26)$$

At the mid-line, the shear strain ψ_x of the beam, for z=0, including the rotation angle of cross-section perpendicular to the mid-line of the form $\theta = \frac{\partial u}{\partial z}$, is presented as shown below:

$$\psi_x = \theta + \frac{\partial w_{\mathbf{0}}}{\partial x} \quad (27)$$

where, θ and $\frac{\partial w_{\mathbf{0}}}{\partial x}$ are the rotation angles with respect to z axis and x axis, respectively.

Substituting ψ_x (Eq. 27) and $\varphi(z)$ (Eq. 24) by their expressions in Equation (26), and after simplification, we obtain the following equation:

$$\varepsilon_x(x,z) = \frac{\partial u_0}{\partial x} - z\frac{\partial^2 w_0}{\partial x^2} + \left(\frac{13}{12}z - \frac{13z^3}{9h^2}\right)\frac{\partial\theta}{\partial x} + \left(\frac{13}{12}z - \frac{13z^3}{9h^2}\right)\frac{\partial^2 w_0}{\partial x^2} \quad (28)$$

The shear deformation $\gamma_{x,z}$ (x,z) is given as follows:

$$\gamma_{xz}(x,z) = \frac{\partial\varphi(z)}{\partial z}\,\psi_x = \left(\frac{13}{12} - \frac{13z^2}{3h^2}\right)\psi_x \quad (29)$$

while the normal stress and the shear stress of Hooke's basic constitutive law are presented as follows:

$$\sigma_{xx}(x) = E(z)\varepsilon_x \quad (30)$$

$$\tau_{xz}(x) = G(z)\gamma_{xz} \quad (31)$$

NUMERICAL COMPARISON AND DISCUSSION OF RESULTS

Comparison of Shear Function Curves

Figures 4 and 5 present the shear function curves of Reddy (1984) and Guenfoud et al. (2016), respectively. It can be seen that the proposed shear function (Figure 6) is in good agreement with those of both Reddy and Guenfoud et al. for square root point's solutions.

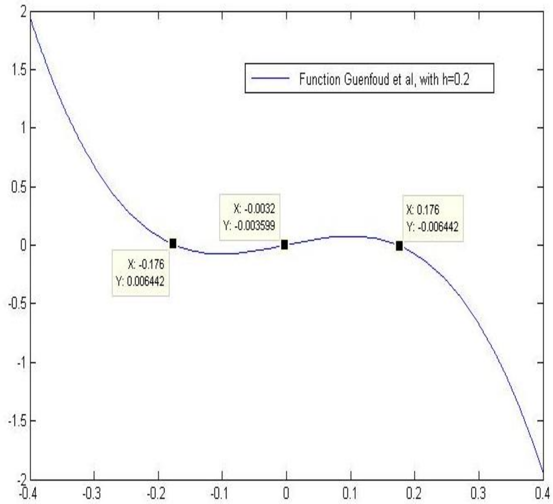

Figure (5): Guenfoud's analytical function curve with square root point solutions

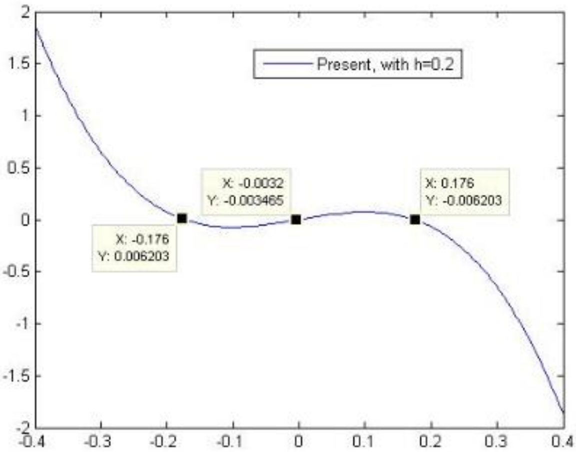

Figure (6): Present proposed new polynomial function curve with square root point solutions

Comparison of Displacement and Variation of Normal and Transverse Shear Stresses of Beam

Considering an illustrative case of the FGM beam with a rectangular cross section (*bxh*) subjected to distributed uniform load, the geometrical and mechanical properties of the studied beam are as follows:

Length L=10m; Height h=0.1m; Width b=0.001m; Load q=1Pa; υ=0.25; E_c=10000GPa; E_m=1000GPa; υ=0.25; L/h=100.

Figure 7 presents the variation of transverse displacement (w) with respect to the power law index (P=5) for the FGM beam under uniform load with L/h=100. It can be seen that the proposed function exhibits displacement results close to those of the other higher-order shear deformation beam theories (Genmfoud's function).

It is shown that there is a significant increase in the displacement at the middle zone of the simply supported beam.

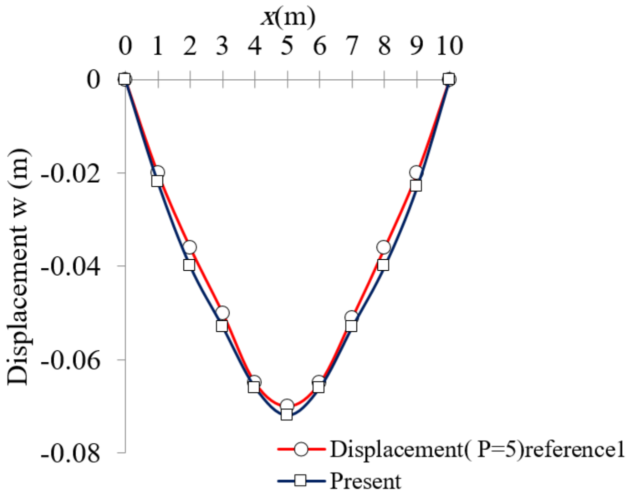

Figure (7): Comparison of displacement (w) of the beam for P=5 and L/h=100

Figure 8 shows the variation of the axial normal stress through the thickness of the FGM beam under uniform load q for L/ h=100. It can be observed that the normal-stress curve through the thickness exhibits a cubic distribution for the higher-order theories used. Furthermore, the normal-stress results predicted using the proposed function are in good agreement with those obtained from Genmfoud's function.

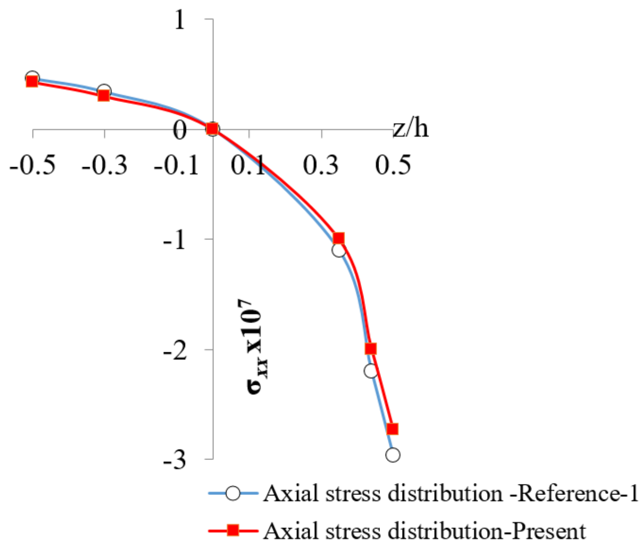

Figure (8): Comparison of axial-stress variation (σ_{xx}[Pa]) *versus* z/h of the beam for P=5 and L/h=100

Figure 9 depicts the variation of the transverse shear stress through the thickness of the FGM beam under uniform load. It can be noted that the maximum value of the transverse shear stress predicted from the proposed function is about 0.75x10^5 Pa, which is similar to that obtained from Genmfoud's function for the studied beam having the power law index P=5 and L/h=100.

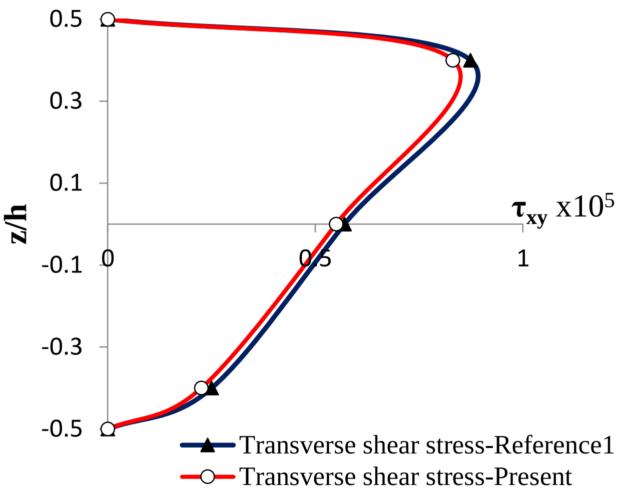

Figure (9): Comparison of transverse shear-stress variation (τ_{xz}[Pa]) *versus* z/h of the beam for P=5 and L/h=100

Considering another illustrative example of the simply supported steel beam subjected to distributed uniform load q, from Equation (21) proposed by Ghugal and Sharma (2011), the maximum transverse displacement at mid- span (x=L/2) for the flexure of thick beams is given by the following expression:

$$w_{c2}\left(x=\frac{L}{2}\right)=-\frac{5qL^4}{384E_x\mathrm{I}}\left(1+1.92(1+\mu)\frac{h^2}{L^2}\right) \qquad (32)$$

where μ is the Poisson's ratio of the beam material.

The properties of the steel beam (IPE 300) considered are as follows:

Length L = 10 m; Cross-section bxh (150mmx300mm); Distributed load q = 5 kN/m (including the self-weight of the beam and the pedestrian load); Type of steel beam: S275; Moment of inertia I=8356cm^4; Poisson's ratio μ=0.3; Elasticity modulus E_x=210GPa.

The results show that the displacement value at mid-span (x=L/2) obtained from Equation (32) ($w_{c2}=0.3718$mm) is similar to that predicted from the proposed model (Eq. 23-a) ($w_{c2}=0.3724$mm). It can be observed that the difference between both values does not exceed 0.2%, which implies the validity of the proposed model and its efficient use in FGM beams and steel constructions.

CONCLUSIONS

Higher-order shear strain new theories were used which include shape functions and stress nullities at the bottom and top faces of the section through the beam thickness. These theories do not require a shear correction coefficient. Timoshenko's theory including the cross-section deformation (shear deformation effect) is added to the displacement field with a linear shape function, while the Euler-Bernoulli classical beam theory (CBT) considers that the cross-sections normal to the mid surface before deformation remain straight and normal to the median surface after deformation. A new polynomial shear function was proposed and introduced on the analytical model of the FGM beam under bending, taking the shear deformations in the displacement field into account.

The results in terms of displacements, deformations, normal and shear stresses obtained with the new polynomial shear function allow to draw the following conclusions:

1. The proposed new polynomial shear function exhibits the best convergence with that found in literature, satisfying the boundary conditions without stresses on the top and bottom surfaces of the simply supported beam.
2. The proposed mathematical model taking into account the shear strains in the displacement field is efficient and consequently provides good accuracy of the predicted solutions for FGM beams under bending.
3. The numerical results, in terms of displacements, axial and shear stresses, compared to those obtained from the literature, are almost similar. Finally, the field component of displacements and the basic constitutive laws are influenced by both the deformation function effect and the shear deformation effect.
4. Different shape functions are used and their determinations are directly influenced by analytical solutions. Thus, the proposed shear function can be used in future studies.

For future works, it is recommended to analyze the proposed model for other materials of beams and shells not used in this study. It is also suggested to investigate FGM structures based on machine learning with reliability and cost optimizations made using the proposed model.

Acknowledgments

Thanks are due to:

- The General Directorate of Scientific Research and Technological Development (DGRSDT), MESRS, Algeria.
- University Mohamed Khider of Biskra, Algeria.

List of Symbols

L, b, h, I: Length, width, thickness, inertia, respectively.

D^*_{11}, F^*_{55} : Bending stiffness, shear stiffness constants of the beam, respectively.

P, q : Power law index, transverse distributed uniform load, respectively.

N, Q, M: Normal force, shear force, moment, respectively.

u(x,z) ; w(x,z): Axial and vertical displacements, respectively.

$\sigma_x ; \tau_{xz}$:Normal stress and shear stress, respectively.

$\varepsilon_x (x, z)$: Normal strain.

$\gamma_{xz} (x, z)$: Shear deformation.

ψ_x: Shear strain.

$\varphi(z)$: Shear function.

θ: Rotation angle of cross-section perpendicular to the mid-line of the beam.

$\varphi(z)\psi_x (x)$: Warping function.

$\frac{\partial}{\partial x};\frac{\partial}{\partial z}$ **:** Operator of first derivation in x,z-directions, respectively.

$\frac{\partial^2}{\partial x^2};\frac{\partial^2}{\partial z^2}$: Second derivation per operator of derivation in x, z-directions, respectively.

Appendix-1

The complete derivation of Eq.23 is as follows.
The functions φ_x and w are independent of the variable y.

$$\frac{\partial \varphi_x}{\partial x} = \frac{\partial \mathrm{M}(x)}{E_x \,\mathrm{I}} = D^*{}_{11} M_x$$

For $0 \leq x \leq L/2$: $\mathrm{M}(x) = -\mathrm{q}\frac{x^2}{2}$; $\varphi_x(x) = -\mathrm{q}\frac{x^3}{6E_x \,\mathrm{I}} + c_1$.

The symmetry of the deformed imposes: $\varphi_x\left(\frac{L}{2}\right) = 0$ => $C_1 = \frac{q}{6E_x\,\mathrm{I}}x^3$ for x = L/2.

Thus,

$\varphi_x(x) = -\mathrm{q}\frac{L^3}{48E_x\,\mathrm{I}}(1 - 8\frac{x^3}{L^3})$.

By reporting the expression of the bending moment M(x) in the equation

$$\frac{\partial M_x}{\partial x} = \frac{1}{F_{55}{}^*}\left(\varphi_x + \frac{\partial w_0}{\partial x}\right) = bhG_{xz}\left(\varphi_x + \frac{\partial w_0}{\partial x}\right)$$

we obtain : $\frac{\partial w_0}{\partial x} = -\left(\varphi_x + \frac{\frac{qL}{2}}{bhG_{xz}}\right)$

It is noted that the slope of deformation at the mid-span of the beam is:

$At\ x = \frac{L}{2}\ ,\ \varphi_x\left(\frac{L}{2}\right) = 0$

Thus, $\frac{\partial w_0}{\partial x}\left(\frac{L}{2}\right) = -\frac{\mathrm{qL}}{2bhG_{xz}}$

By substituting the expression of φ_x below in the following equation and after integration, we obtain the final expression of the displacement:

$$w_0(x) = \int_0^{\frac{L}{2}} -(\varphi_x + \frac{\mathrm{qL}}{2bhG_{xz}})\,\mathrm{dx} = -\int_0^{\frac{L}{2}}(\frac{qL^3}{48E_x\,\mathrm{I}}\left[1 - 8\frac{x^2}{L^2}\right] + \frac{qL}{2bhG_{xz}})\,\mathrm{dx}$$

$$\varphi_x(x) = -\frac{qL^3}{48E_x\,\mathrm{I}}\left[1 - 8\frac{x^3}{L^3}\right] = -\frac{qL^3}{48\mathrm{b}}D^*{}_{11}\left[1 - 8\frac{x^3}{L^3}\right]$$

The final expression is presented by Eq. (23).

The maximum value is evaluated at (*x*=L/2) by Eq. (23-a).

REFERENCES

Aydogdu, M., and Taskin, V. (2007). “Free-vibration analysis of functionally graded beams with simply supported edges”. Materials & Design, 28, 1651-1656. https://doi.org/10.1016/j.matdes.2006.02.007

Benatta, M.A., Mechab, I., Tounsi, A., and Adda Bedia, E.A. (2008). “Static analysis of functionally graded short beams including warping and shear deformation effects”. Computational Materials Science, 44, 765-773. https://doi.org/10.1016/j.commatsci.2008.05.020

Gandhe, G.R., Pankade, P.M., Tupe, D.H., and Taur, P.G. (2018). “Higher-order computational method for static flexural analysis of thick beam”. Procedia-Manufacturing, 20, 493-498. https://doi.org/10.1016/j.promfg.2018.02.073

Ghugal, Y.M., and Sharma, R. (2011). “A refined shear-deformation theory for flexure of thick beams”. Latin American Journal of Solids and Structures, 08, 183-193. https://doi.org/10.1590/S1679-78252011000200005

Ghugal, Y.M., and Ajay, G.D. (2012). "Flexure of thick beams using refined shear deformation theory". International Journal of Civil and Structural Engineering, 3 (2), 321-335. doi:10.6088/ijcser.201203013031

Guenfoud, H., Ziou, H., Himeur, M., and Guenfoud, M. (2016). "Analyses of a composite functionally graded material beam with a new transverse shear deformation function". Journal of Applied Engineering Science & Technology, 2 (2), 105-113. https://revues.univ-biskra.dz/index.php/jaest/article/view/1898

Kadoli, R., Akhtar, K., and Ganesan, N. (2008). "Static analysis of functionally graded beams using higher-order shear deformation theory". Applied Mathematical Modeling, 32 (12), 2509-2525. https://doi.org/10.1016/j.apm.2007.09.015

Li, M., Guedes Soares, C., and Yan, R. (2020). "A novel shear deformation theory for static analysis of functionally graded plates". Composite Structures, 250. https://doi.org/10.1016/j.compstruct.2020.112559

Li, X.-F. (2008). "A unified approach for analyzing static and dynamic behaviors of functionally graded Timoshenko and Euler–Bernoulli beams". Journal of Sound and Vibration, 318, 1210-1229. https://doi.org/10.1016/j.jsv.2008.04.056

Lu, C.F, Chen, W.Q., Xu, R.Q., and Lim, C.W. (2008). "Semi-analytical elasticity solutions for bi-directional functionally graded beams". International Journal of Solids and Structures, 45 (1), 258-275. https://doi.org/10.1016/j.ijsolstr.2007.07.018

Reddy, J.N. (1984). "Simple higher-order theory for laminated composite plates". Journal of Applied Mechanics, 51 (4), 745-752. https://doi.org/10.1115/1.3167719

Sayyad, A.S., and Ghugal, Y.M. (2011). "Flexure of thick beams using new hyperbolic shear deformation theory". International Journal of Mechanics, 5 (3), 113-122.

Şimşek, M. (2009). "Static analysis of a functionally graded beam under a uniformly distributed load by Ritz method". International Journal of Engineering and Applied Sciences, 1 (3), 1-11. https://dergipark.org.tr/en/pub/ijeas/issue/23571/251092

Zaoui, F.Z., Hanifi, H., Lemya, A., Younsi A., Meradjah, M., Tounsi A., and Ouinas, D. (2017). "Free-vibration analysis of functionally graded beams using a higher-order shear". Mathematical Modeling of Engineering Problems, 4, 7-12. https://doi.org/10.18280/mmep.040102

Zheng, Zhong, and Tao, Yu. (2007). "Analytical solution of a cantilever functionally graded beam". Journal of Composites Science and Technology, 67, 481-488. https://doi.org/10.1016/j.compscitech.2006.08.023

Ziou, H., Guenfoud, H., and Guenfoud, M. (2016). "Numerical modeling of a Timoshenko's FGM beam using the finite element method". International Journal of Structural Engineering, 7, 239-261. doi:10.1504/IJSTRUCTE.2016.077719

Ziou, H., Guenfoud, M., and Guenfoud, H. (2021). "A simple higher-order shear deformation theory for static-bending analysis of functionally graded beams". Jordan Journal of Civil Engineering, 15 (2), 209-224.